Acta Neuropathol (Berl) (1984) 65:128–137

Acta Neuropathologica

Axonopathy and Microangiopathy in Chronic Alloxan Diabetes*

H.C. Powell and R.R. Myers
Depts. of Pathology, Anesthesia, and Neurosciences, University of California, San Diego, La Jolla, CA 92093, USA

Summary. A significant reduction in the myelinated nerve fiber population was observed during quantitative electron-microscopic examination of peripheral nerves in chronic alloxan diabetic rats. Dystrophic axonal abnormalities and regenerating fibers were more numerous in diabetics than age-matched controls. Schwann cells showed reactive changes including prominent pi granules of Reich and intracytoplasmic filament accumulation. Enumeration of these alterations, however, revealed no significant difference from controls. Endoneurial macrophages in diabetic rats were also filled with lamellar intracytoplasmic inclusions characteristic of a chronic neuropathy. Quantitation of pathologic lesions in teased nerve fibers confirmed the preponderance of axonal over demyelinative disease and showed demyelination to be segmental.

Microangiopathy was noted throughout the vasa nervorum of diabetic rats, and quantitative electron microscopy showed endothelial proliferation with doubling of the number of endothelial cells and proportional capillary mural thickening. Swollen, reactive endothelial cells appeared to efface the vascular lumen and may impair capillary perfusion. These microcirculatory changes, in the presence of biochemical and rheologic disturbances may contribute to tissue hypoxia and underly the loss of axons in experimental diabetic neuropathy.

Key words: Quantitative – Electron microscopy – Microangiopathy – Pi granules – Schwann cells

Introduction

Of the several animal models for diabetic neuropathy, alloxan-induced diabetes has been especially useful in reproducing chronic complications, such as axonopathy, demyelination, and microangiopathy of the vasa nervorum [22]. This model may thus be used to answer such questions as to whether axonal dystrophy or demyelination is the primary lesion of the nerve fiber and if accumulation of pi granules, reported both in human diabetics [2] and in genetically diabetic mice [4], is pathologically significant.

A decade ago, diabetic neuropathy was considered to be attributable primarily to a disorder of the Schwann cell. This view was based upon findings of segmental demyelination in human diabetic nerves [35] and on the demonstration of high concentrations of sorbitol and fructose: putative products of Schwann cell metabolism, in diabetic nerves [8, 33]. Furthermore biochemical analysis of alloxan diabetic rabbit nerves [32] revealed an overall reduction in myelin content. In recent years, however, there has been greater emphasis on the axon as a primary focus of injury, and demyelination may be both primary and secondary [1, 5, 6, 29, 34, 39]. There is morphometric evidence of primary axonopathy from neuropathologic studies of C57BL/Ks (db/db) mice [11, 30]. The purpose of this paper is to report findings of teased nerve fiber examination and quantitative electron microscopy which suggest that axonopathy is the principal nerve fiber lesion in chronically alloxan-diabetic rats and to emphasize proliferative changes in the vasa nervorum associated with mural thickening of the microvasculature.

Materials and Methods

Male Lewis rats, weighing 350–400 g, were used in this study. Alloxan diabetes was induced by i.v. injection of alloxan monohydrate 42–44 mg/kg body weight. These animals and the controls then received a standard laboratory diet. Blood sugars were recorded at 2-week intervals throughout the study, and animals which did not become diabetic were excluded from the study. Altogether 38 rats were used in this study consisting of 17 diabetics and 21 controls.

* Supported in part by NS-14162 and NS-09053 from the National Institute for Neurological and Communicative Disorders and Stroke and the Veterans Administration Research Service

Offprint requests to: Dr. H.C. Powell, Dept. of Pathology, M-012D, University of California, San Diego, La Jolla, CA 92093, USA

Neuropathology

Under deep nembutal-induced anesthesia 2.5% phosphate-buffered glutaraldehyde was infused into the abdominal aorta of the rat. The sciatic nerves were dissected and immersed in glutaraldehyde overnight prior to processing for electron microscopy. Approximately 2.5 cm long portions were obtained from the mid-thigh region. Portions of the sciatic nerves were embedded in araldite, and 1-μm sections from the blocks were examined microscopically. Teased nerve fibers were prepared by infiltrating the nerves with low viscosity resin and then isolating single fibers with dissecting needles. One hundred teased nerve fibers were prepared from each nerve. Prior to teasing each nerve was desheathed and then broken into several clumps from which equivalent numbers of fibers were selected. Teasing was carried out in nerves from 13 "control" rats and nine surviving alloxan-diabetic rats from a group of animals that were maintained for 16–18 months.

For quantitative electron microscopy blocks were selected after prescreening to exclude any which contained only fatty or adventitial tissue, and four were randomly chosen from the blocks available on each of 16 animals as described previously [24]. Prior screening was also used to identify edema, Renaut bodies, or fibrosis. Each

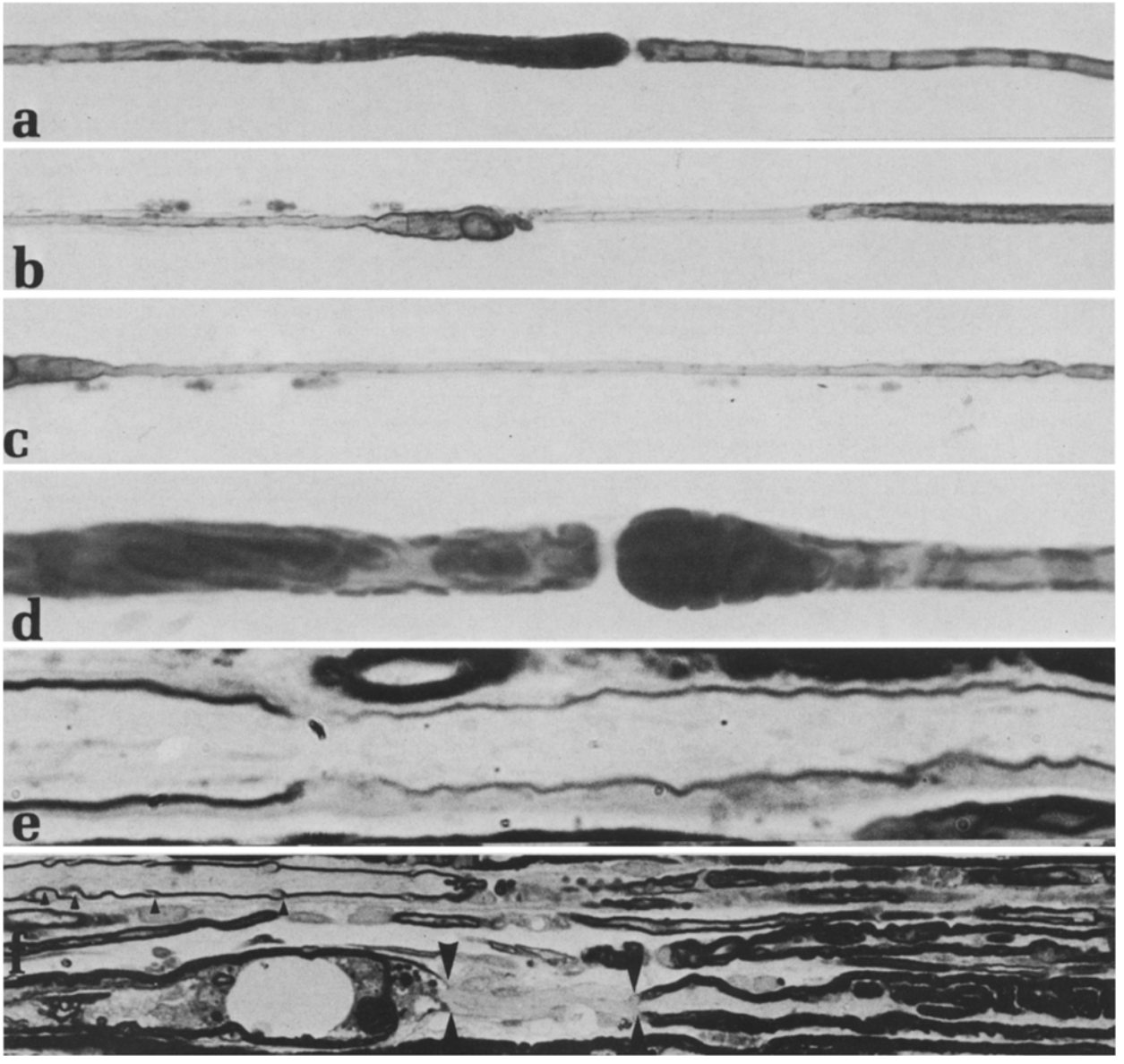

Fig. 1a–f. Axonal and demyelinative changes in alloxan-diabetic neuropathy. **a** Paranodal axonal swelling. **b–c** Focal axonal swelling, myelin ovoids consistent with nerve fiber degeneration and a shortened thinly myelinated internodal segment characteristic of regeneration. **d** Paranodal axonal swelling. **e** Two adjacent internodal segments of a myelinated axon reveal abnormally thin myelin sheaths reflecting different stages of remyelination. **f** A completely demyelinated segment is marked by *large arrowheads* at the node of Ranvier. A nearby remyelinating axon shows numerous Schmidt-Lanterman (*S-L*) clefts (*small arrowheads*). S-L clefts increase during nerve fiber injury. Magnifications **a–d**, teased nerve fibers preserved in low viscosity resin, 250 n, 250 n, 250 n, 1,000 n. **e–f** 1-μm-thick araldite section stained with paraphenylene diamine, 1,000 n

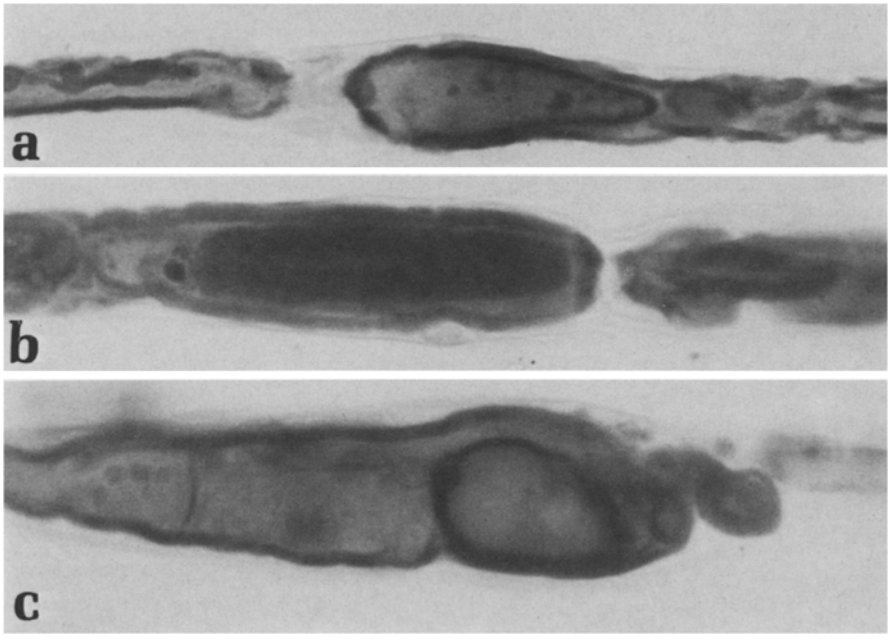

Fig. 2a–c. Dystrophic axons in alloxan-diabetic rat nerve. **a** Paranodal swelling with densely packed axoplasm. **b** An elliptically shaped axonal inclusion consistent with a glycogenosome. **c** Focal axonal swelling with densely staining axoplasm exhibiting a "ground-glass" appearance. ×1,800

of the 64 blocks was assigned a code number so that the quantitative analysis could be conducted "blind". Blocks were trimmed so that the size of the block face was approximately 0.5 mm^2, and thin sections cut and stained with uranyl acetate and lead citrate. Sections were examined in a Zeiss 9 electron microscope in which metered X and Y co-ordinates on the stage drive permitted the operator to select areas for micrography guided by random numbers tables. In the event that the grid square was not uniformly covered by a tissue section, the operator was instructed to continue using the table until a technically satisfactory micrograph was obtained. The use of a large thin section was designed to provide an adequate number of fields and to reduce the possibility of taking the same picture twice. From each section four electron micrographs of the same magnification (×1,000) were taken, and a total of 16 randomly selected electron micrographs represented each of the 16 animals studied. The 256 electron micrographs thus obtained were then examined "blind" for analysis of pi granules, interstitial macrophages, onion bulb formation, enumeration of the myelinated fibers, and measurement of fiber size. These animals survived for 24 months and were the subject of a previous quantitative electron-microscopic study of intra-axonal glycogen accumulation [24].

To study microangiopathy separate electron micrographs were prepared from nerves of 4 alloxan diabetic animals and four controls. Thin sections were made in randomly selected blocks and micrographs were obtained by moving the stage drives as far as possible in the same direction and then scanning the grid squares in sequence. As each vessel was identified an electron micrograph was taken and the number recorded. No picture was taken if the vessel's profile was obscured by artifacts such as folds or breaks in the section. Full size (8 × 11 inch) prints were made from the negatives and the inner and outer circumference of each capillary was measured with a planimeter. Qualitative assessments of the extent of endothelial proliferation were also recorded. Student's unpaired "t" test was used in statistical analysis of the findings.

Results

Teased nerve fibers showed various axonal dystrophic changes including para-axonal swelling (Figs. 1, 2),

Table 1. Teased nerve fibers (100 fibers/specimen)

	Mean	SD	No.	SE	Probability
Dystrophic axons					
D	10.7	5.3	9	1.8	$p<0.005$
C	2.1	1.8	13	0.5	
Demyelination					
D	1.8	1.5	9	0.5	$p<0.01$
C	0.5	0.8	13	0.2	

SD, standard deviation
SE, standard error
D, Diabetic
C, Control

focal axonal swellings some of which were uniformly dense, while others had a "ground glass" appearance (Fig. 2), and myelin ovoids consistent with nerve degeneration. Shortened internodes (Fig. 1 b) and thin myelin sheaths (Fig. 1 b, c, e) were also noted and are recognized as features consistent with regeneration. Segmental demyelination (Fig. 1 f). was seen both in araldite sections and teased fibers, but occurred less frequently than primary axonal pathology (Table 1).

Various abnormalities were noted during routine ultrastructural examination. Swollen Schwann cells were sometimes observed with electron-lucent cytoplasm and disintegrating organelles (Fig. 3). Since not all Schwann cells were affected in this way, the change is not considered to be associated with a polyol abnormality. Other Schwann cell abnormalities included filamentous dysplasia of the inner loop (Fig. 4), supernumerary basal lamina (Fig. 5), "mi-

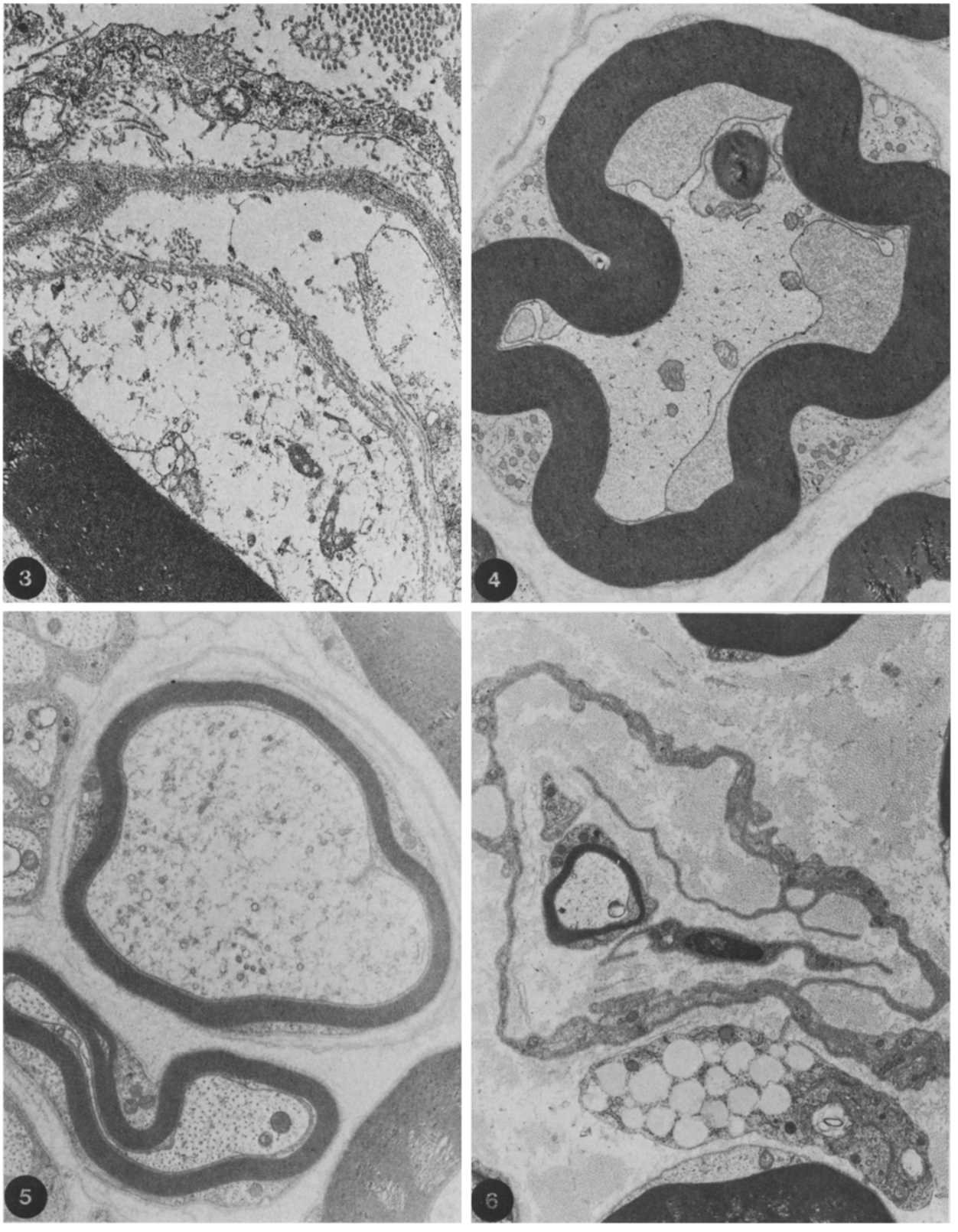

Figs. 3–6. (for detailed legends, see p. 132)

nor" onion bulb formation (Fig. 6), and perikaryonal swelling with masses of intermediate cytoplasmic filaments and endoplasmic reticulum (Fig. 7). These dystrophic Schwann cell changes are non-specific and probably represent a response to axonal injury. In this context "minor" onion bulbs constitute further evidence of a response to axonopathy. Minor or "thin" onion bulbs appear during regeneration in chronic axonopathies and also are seen in aging nerve. In the present study they were found around 0.22% of myelinated fibers in diabetic rats as compared to 0.05% in controls. Membrane-bound, lamellar lipid inclusions, identical to pi granules in Schwann cells were present in endoneurial macrophages in diabetic nerves (Figs. 8, 9). Lipid inclusions were also observed in diabetic macrophages (Fig. 6). Although there was no significant differences in the overall number of macrophages (Table 2), diabetic macrophages were packed with this material. As in the case of the Schwann cells, the findings are suggestive of chronic neuropathy. Finally, a composite histogram was constructed from measurements of myelinated fiber size in 256 coded electron micrographs (Fig. 10). The findings revealed that the myelinated axons were fewer in diabetic rats than in controls. Since we did not detect nerve swelling due to edema and in the absence of Renaut bodies and subperineurial fibrosis by light microscopy, we assume that the reduction in fiber density is not an artifact. Attempts were made to quantify microangiopathy of the vasa nervorum in diabetic rats. Viewed by electron microscopy, the most notable change appeared to be endothelial proliferation, involving not only cellular proliferation and reduplication of basal lamina, but also substantial swelling of endothelial cytoplasm. Swollen endothelial cells bulged into the lumina of capillaries, sometimes effacing them. Swollen endothelial cytoplasm appeared qualitatively normal. Assessment of endothelial proliferation was performed in different ways. Firstly, semi-quantitative estimation of proliferation was carried out on randomized electron micrographs. Vessels were graded from 0 (normal) to + + + +, depending on the extent of endothelial proliferation. A second, quantitative

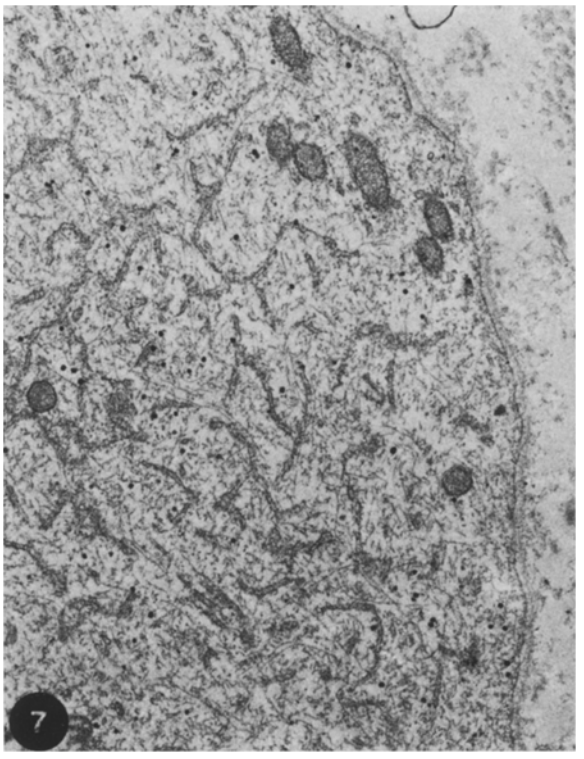

Fig. 7. Swollen, reactive Schwann cell cytoplasm packed with uniformly dispersed intermediate cytoplasmic filaments and cisternae of endoplasmic reticulum glycogen granules are scattered throughout the cell. × 15,000

method, applied to these electron micrographs involved measurement of the circumference of the inner layer of the capillary endothelium. The area of the inner endothelial layer was then calculated, and the endothelial area and vascular luminal areas were compared in alloxan-diabetic rats and controls (Table 3). Thirdly, enumeration of endothelial cells was attempted by counting their nuclei in coded electron micrographs obtained in a randomized survey. Semiquantitative estimation of capillary endothelial proliferation showed a significantly greater endothelial cytoplasmic size in diabetic animals, and subsequent measurement of endothelial circumference revealed it to be approximately double in the diabetic rats (Table 3). The endothelial cell population, also deter-

Fig. 3. The Schwann cell at the base of this electron micrograph has swollen electron-lucent cytoplasm with scattered disintegrating organelles. There is onion bulb formation with cytoplasm of a supernumerary Schwann cell adjacent to the abnormal cell. × 11,400

Fig. 4. The principal abnormality in this myelinated fiber is filamentous dysplasia of the inner loop of Schwann cell cytoplasm filling the periaxonal region. × 7,600

Fig. 5. Swollen degenerating axoplasm with empty vesicles and fibrillar debris. The affected fiber is surrounded by thin layers of redundant basal lamina. × 8,550

Fig. 6. Minor onion bulb formation around a thinly myelinated axon. The macrophage at the *bottom* of the picture is filled with lipid droplets. × 5,250

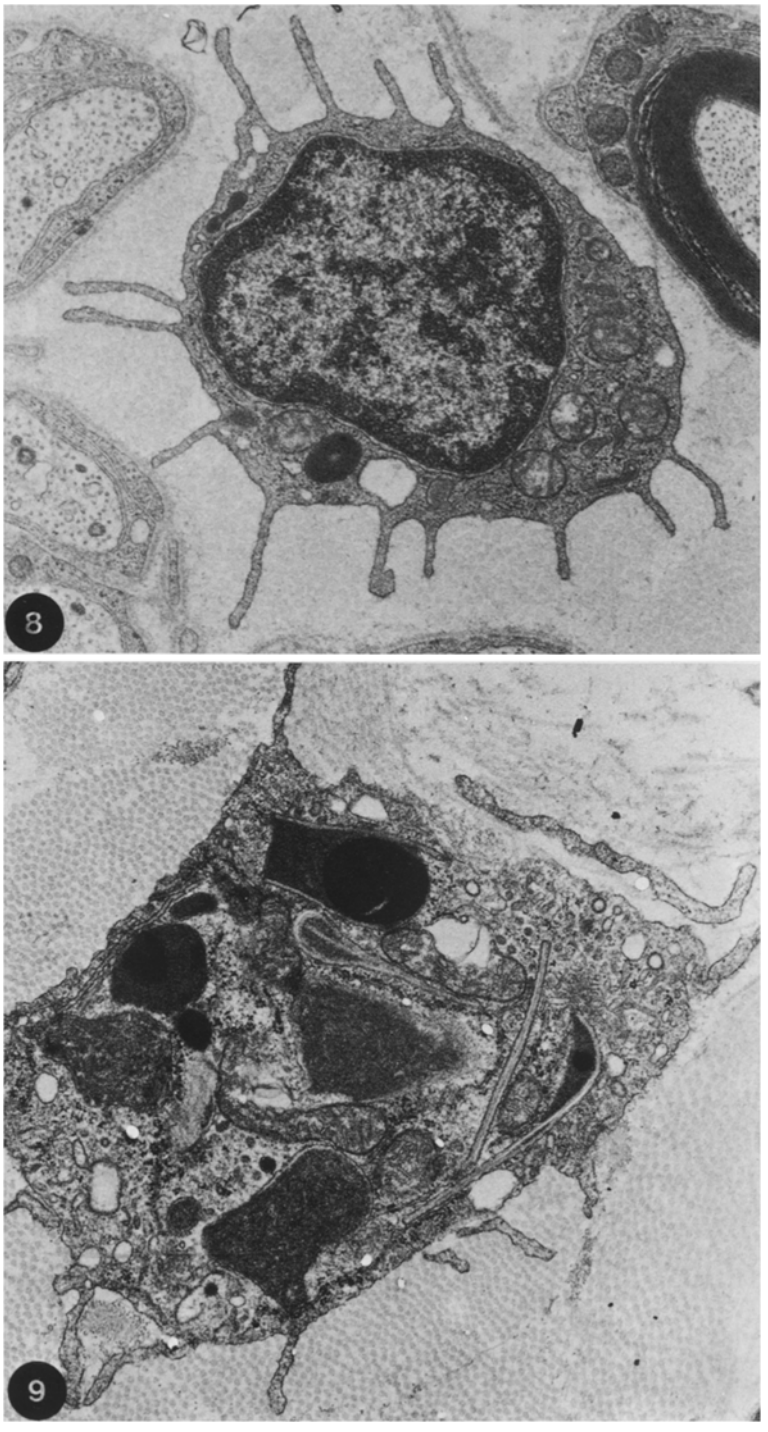

Figs. 8, 9. Macrophage from a control (**Fig. 8**) and a diabetic animal (**Fig. 9**). Macrophages in the diabetic are characteristically filled with lamellar inclusions and darkly staining lysosomal bodies. ×10,000

mined by counting their nuclei, was almost twice as numerous in diabetics (Table 3).

Discussion

The principal neuropathologic change in alloxan-diabetic rats was a diffuse loss of myelinated axons (Table 2). Schwann cells filled with lamellar lipid inclusions, although conspicuous in diabetic neuropathy, were not significantly more numerous than similar cells in age-matched controls. Thus, there is no ultrastructural evidence for a lipid metabolic defect in Schwann cells in this model. Interstitial macrophages, packed with lamellar (Fig. 9) inclusions were also

Table 2. Quantitative electron microscopy

	Mean	SD	No.	SE	Probability
Myelinated axons					
D	346.0	48.4	8	17.1	$p<0.01$
C	431.0	75.8	8	26.8	
Schwann cells					
D	193.3	69.8	8	24.7	$p>0.05$
C	240.3	64.2	8	22.7	
Pi granules					
D	5.38	3.0	8	1.06	NS
C					
Endoneurial macrophages					
D	7.9	5.2	8	1.8	NS
C	6.0	4.0	8	1.4	

NS, not significant

Table 3. Microangiopathy of the vasa nervorum in alloxan-diabetic neuropathy

	Mean	SD	SE	No.	Significance
1. Endothelial circumference (μm^2)					
Diabetic	192.25	101.83	28.24	13	
Control	106.28	34.40	9.93	12	$p<0.01$
2. Endothelial luminal diameter					
Diabetic	36.01	8.57	2.38	13	NS
Control	42.97	11.89	3.43	12	
3. Endothelial proliferation in endoneurial microcirculation					
Diabetic	2.769	0.599	0.166	13	
Control	0.667	0.779	0.225	12	$p<0.001$
4. Endothelial nuclei per section					
Diabetic	2.33	1.37	0.40	12	
Control	1.33	0.89	0.26	12	$p<0.005$

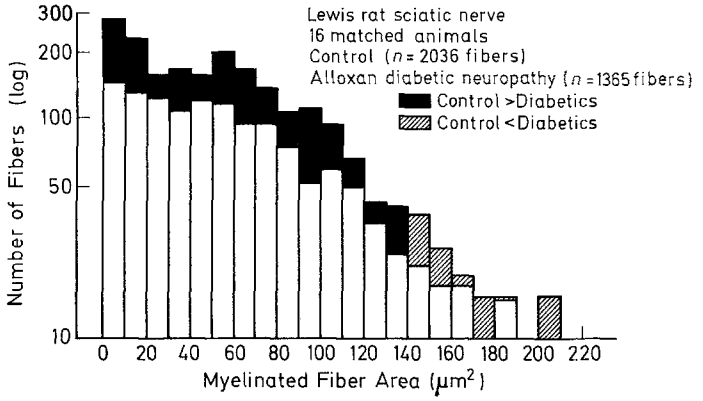

Fig. 10. Nerve fiber areas from transverse sections of rat sciatic nerve. Two groups of animals, control and alloxan-diabetic, are displayed on this semi-logarithmic histogram which plots the *number of fibers* (log) vs. *myelinated fiber area* (in 24 bins from 0–240 μm^2). All transversely cut myelinated fibers were counted from randomly selected, paired electron micrographs. The *solid black bars* in the histogram represent the difference between groups in which the number of fibers in the control group was greater than the number from the diabetic group within that area bin. The *hashed bars* represent the converse; the number of fibers in the diabetic group exceeded the control group for that bin. Note the greater number of fibers in the control group for areas less than 140 μm^2 but a greater number of large fibers above 140 μm^2 in the diabetic group. A paired Student's *t*-test, bin by bin for all fibers, indicated a significantly greater number of fibers in the control group ($p=0.001$)

prominent in the diabetic endoneurium, but this appeared to be a qualitative change since interstitial macrophages were not significantly increased overall. Signs of increased Schwann cell lysosomal activity and similar alterations of macrophages are non-specific changes characteristic of a chronic neuropathy and consistent with the observed loss of myelinated fibers. In the following paragraphs the findings in axons, Schwann cells, and the endoneurial interstitium in alloxan-diabetic neuropathy will be discussed.

Axons

A count of myelinated nerve fibers in diabetic rats and age-matched controls disclosed a statistically significant reduction in this population in diabetic rat nerves (Table 2). The number of myelinated axons identified in micrographs of the same magnification from diabetic rat nerve was considerably fewer (1,368) than in age-matched controls (3,026), and the difference was significant ($p=0.001$). Nerve fiber reduction appeared to involve myelinated fibers in all but the larger categories (Fig. 10), and increased collagen was interposed between fibers in the endoneurial interstitium. No swelling of the nerves was detected microscopically and "Structureless space", as described by Jakobsen [13] in streptozotocin rats with nerve edema, was not observed in electron micrographs, nor was there any sign of edema or fibrosis in 1-μm-thick sections examined by light microscopy. No specific changes appeared within the axoplasm; however, masses of glycogen and polyglucosan accumulated in axonal mitochondria. Although this change is non-specific, it is pathologically significant, in that these inclusions occurred twice as commonly as in age-matched controls. An increase in axonal glycogenosomes has also been reported in diabetic mutant mice [31] and in human nerves [37, 39]. While its pathogenesis in peripheral neuropathy is not presently understood, attempts to explain it may be relevant to the mechanism of axonal loss. Glycogen storage within mitochondria is not a uniquely neurologic phenomenon; it can be reproduced in experimental

anoxic states in the canine heart [3] and was first noticed during pathologic studies of human ischemic heart disease [28]. It appears that when tissue oxygen concentrations are insufficient, glycogen is stored in the outer compartments of mitochondria and accumulates in proportion to the oxygen deficit. When accumulation of intramitochondrial glycogen becomes extensive in peripheral nerve, transformation of glycogen into polyglucosan deposits occurs [24]. These inclusions may become quite large, filling the greater part of the axon. These and other dystrophic changes may be responsible for the preponderance of large diameter fibers among diabetic rats.

Myelin and Schwann Cells

Morphologic changes of Schwann cells in chronic alloxan-diabetic neuropathy appeared to be reactive, and no specific mechanism of primary demyelination was elicited. The swelling of Schwann cell perikarya with masses of intermediate cytoplasmic filaments has not been reported at earlier stages of diabetic neuropathy, but has been described in animals with distal axonopathy due to 2,5 hexanedione (2,5 HD) neurotoxicity after several months of experimental intoxication [23]. The primary lesion in 2,5 HD neuropathy involves the peripheral axon, and demyelination, when it occurs, appears to be secondary [9], showing a temporal and a topographic distribution consistent with a delayed effect of axonal degeneration. Periaxonal filament accumulation (Fig. 5) may also be observed in chronic neuropathy [12]. This non-specific change of the adaxonal compartment of Schwann cells was noteworthy in alloxan-diabetic rats, in which it sometimes circumscribed the entire axon, while in aging controls the change was focal, involving a smaller portion of the periaxonal region.

Accumulation of pi granules in the Schwann cell cytoplasm has been noted by other investigators in both human [2] and experimental diabetic neuropathy [4] and has been viewed as possibly indicative of a disorder of lipid metabolism [36]. Although the change was prominent in diabetic Schwann cells and occurred more frequently (Table 2), the difference was not significant between alloxan-diabetic rats and age-matched controls, and it may be concluded that this, too, is a secondary change associated with chronic abnormality of the axon. Prominent pi granule accumulation in Schwann cells has already been described in the course of chronic neuropathies in which axonal degeneration is the principal disorder [27]. A possibly related change occurred in endoneurial macrophages, which in diabetic rats were always packed with multi-lamellar and homogeneous lipid inclusions. This abnormality probably reflects an increased breakdown of myelin in the course of axonal degeneration, and the findings are not supportive of a lipid metabolic defect. The morphologic findings, while supportive of the concept of secondary demyelination, do not rule out the possibility of primary demyelination in this model.

Microangiopathy of the Vasa Nervorum

Morphometric analysis of endoneurial blood vessels revealed significant changes in the vasa nervorum of alloxan-diabetic neuropathy. Changes in the basal laminae have already been reported [22], and the objective of these morphometic studies was to analyze proliferative changes observed in the endothelial layer. As a result of these alterations the normal smooth flattened appearance of endothelium, forming a thin capillary wall, is replaced by plump endothelial cells whose cytoplasm bulges into the lumen [22]. Both the outer circumference of the endothelial layer and the luminal circumference were measured in test animals and controls. The area enveloped by the basal lamina was twice as great in the diabetics as in controls, while the capillary lumina showed no significant difference in area (Table 3). A separate "semi-quantitative" assessment was performed on coded electron micrographs which were graded for endothelial proliferation and once again significant differences were appreciated (Table 3). The importance of endothelial proliferation is that increased numbers of abnormally large endothelial cells tend to reduce luminal area relative to capillary size and may have an impact on microvascular blood flow. Endothelial proliferation has been described in human diabetic neuropathy [2, 10] and accelerated turnover of endothelial cells occurs in other tissues [37]. It is one of several microcirculatory disturbances including increased concentrations of glycosylated hemoglobin [26], increased blood viscosity [18], and decreased concentrations of 2–3 diphosphoglycerate [7]. The net effect of these changes is tissue hypoxia, and the problem may be aggravated further by reduced nerve blood flow [21].

Peripheral nerve receives its blood supply from two principal sources. Firstly, axial vessels branching from major arteries pass along the shank of the vessel perfusing the center of each fascicle. Secondly, a richly anastomosing network of small vessels envelopes each fascicle and individual vessels pass obliquely through the perineurium to gain access to the endoneurial contents [15, 16]. Penetration of the semi-rigid perineurial sheath predisposes these vessels to compression in conditions in which the sheath is distended, such as increased endoneurial fluid pres-

sure [17, 20]. Studies of nerve compliance reveal that the perineurium tends to resists distension, and that relatively modest (i.e., 2–3 fold) increases in pressure can be associated with reduced nerve blood flow [21]. Although increased fluid pressure rarely occurs in experimental diabetic neuropathy [25], a possible ischemic mechanism has been identified in human diabetic neuropathy in which a combination of endothelial proliferation, basal laminar thickening, and reduplication increases the size of vessel walls [38]. When those thickened vessels pass through the perineurium, in which substantial basal laminar thickening occurs [14], the net effect is a reduction in luminal diameter, as shown in biopsy material from chronically diabetic patients (Powell et al., unpublished data). These structural abnormalities may be compounded by alteration in blood viscosity, associated with glycosylation of hemoglobin [26] and of red cell membranes [19] which is associated with increased blood viscosity [18]. These changes augmented by episodic depressions of 2–3 diphosphoglycerate [7] give rise to tissue hypoxia.

The non-specific abnormalities of axon and Schwann cells, accompanied by chronic myelinated nerve fiber loss in these alloxan-diabetic rats, may be due in part to chronic microangiopathy in which there is structural alteration of vessels and functional disturbance of the microcirculation, the cumulative effects of which include ischemic damage to nerve fibers.

References

1. Behse F, Buchthal F, Carlsen F (1977) Nerve biopsy and conduction studies in diabetic neuropathy. J Neurol Neurosurg Psychiatry 40:1072–1082
2. Bischoff A (1980) Morphology of diabetic neuropathy. Horm Metab Res [Suppl] 9:18–28
3. Buja LM, Ferrans VJ, Levitskey S (1972) Occurrence of intramitochondrial glycogen in canine myocardium after prolonged anoxic cardiac arrest. J Mol Cell Cardiol 4:237–254
4. Carson KA, Bossen EH, Hanker JS (1980) Peripheral neuropathy in mouse hereditary diabetes mellitus. II. Ultrastructural correlates of degenerative and regenerative changes. Neuropathol Appl Neurobiol 5:361–374
5. Clements RS (1979) Diabetic neuropathy. New concepts of its etiology. Diabetes 28:604–611
6. Clements RS (1982) Pathogenesis of diabetic neuropathy. NY State J Med 82:864–872
7. Ditzel J (1980) Affinity hypoxia as a pathogenic factor of microangiopathy with particular reference to diabetic retinopathy. J Acta Endocrinol [Suppl] 238:39–55
8. Gabbay KH, Merola LO, Field RA (1966) Sorbitol pathway: presence in nerve and cord with substrate accumulation in diabetes. Science 151:209–210
9. Griffin JW, Price DL (1981) Segmental demyelination in experimental IDPN and hexacarbon neuropathies. Evidence for an axonal influence. Lab Invest 45:130–141
10. Grover-Johnson N, Baumann FG (1982) Neuropathology in diabetes: general aspects with emphasis on the nervous system. NY State J Med 82:860–863
11. Hanker JS, Ambrose WW, Yates PE, Koch GG, Carson KA (1980) Peripheral neuropathy in mouse hereditary diabetes mellitus. J Acta Neuropathol (Berl) 51:145–155
12. Hirano A, Dembitzer HM (1976) Eosinophilic rod-like structure in myelinated fibers of hamster spinal roots. Neuropathol Appl 2:225–232
13. Jakobsen J (1978) Peripheral nerves in early diabetes. Expansion of the endoneurial space as a cause of increased water content. Diabetologia 14:113–119
14. Johnson PC, Brendel K, Meezan E (1981) Human diabetic perineurial cell basement membrane thickening. Lab Invest 44:265–270
15. Lundborg G (1975) Structure and function of the intraneural microvessels as related to trauma, edema formation and nerve function. J Bone Joint Surg [Am] 57:938–948
16. Lundborg G (1979) The intrinsic vascularisation of human peripheral nerves – Structural and functional aspects. J Hand Surg 4:34–41
17. Lundborg G, Myers RR, Powell HC (1983) Increased endoneurial fluid pressure in experimental entrapment neuropathy. J Neurol Neurosurg Psychiatry 46:1119–1124
18. McMillan DE (1982) Further observations on serum visosity changes in diabetes mellitus. Metabolism 31:274–278
19. Miller JA, Pizzighella S, Gravallese E, Bunn HF (1980) Nonenzymatic glycosylation of erythrocyte membrane proteins. Relevance to diabetes. J Clin Invest 65:896–901
20. Myers RR, Powell HC, Shapiro HM, Costello ML, Lampert PW (1980) Changes in endoneurial fluid pressure, permeability, and peripheral nerve ultrastructure in experimental lead neuropathy. Ann Neurol 8:392–401
21. Myers RR, Mizisin AP, Powell HC, Lampert PW (1982) Reduced nerve blood flow in hexachlorophene neuropathy. Relationship to elevated endoneurial fluid pressure. J Neuropathol Exp Neurol 41:391–399
22. Powell HC, Knox D, Lee S (1977) Alloxan diabetic neuropathy. Electron microscopic studies. Neurology (Minn) 27:60–66
23. Powell HC, Koch T, Garrett R, Lampert PW (1978) Schwann cell abnormalities in 2,5 hexanedione neuropathy. J Neurocytol 7:517–528
24. Powell HC, Ward HW, Garrett RS (1979) Glycogen accumulation in the nerves and kidneys of chronically diabetic rats. A quantitative electron-microscopic study. J Neuropathol Exp Neurol 38:114–127
25. Powell HC, Costello ML, Myers RR (1981) Galactose neuropathy. Permeability studies, mechanism of edema and mast cell abnormalities. Acta Neuropathol (Berl) 55:89–95
26. Powell HC, Ivor LP, Costello ML, Wolf PL (1982) Elevated hemoglobin A_I in streptozotocin diabetes and in rats with sucrose and galactose diets. Clin Biochem 15:133–137
27. Powell HC, Lampert PW (1983) Peripheral neuropathies. In: Rosenberg R, Schochet S (eds) Clinical neurosciences, chapt 9, sect III. Churchill Livingstone, Edinburgh Harlow New York, pp 325–362
28. Rosai J, Lascano EF (1970) Basophilic (mucoid) degeneration of the heart. Am J Pathol 61:99–115
29. Said G, Slama G, Selva J (1983) Progressive centripetal degeneration of axons in small fiber type diabetic polyneuropathy. A clinical and pathologic study. Brain 106:791–807
30. Sima AAF, Robertson DM (1979) Peripheral neuropathy in the diabetic mutant mouse. An ultrastructural study. Lab Invest 40:727–732
31. Sharma AK, Thomas PK, Gabriel G, Stolinski C, Dockery P, Hollins GW (1983) Peripheral nerve abnormalities in the diabetic mutant mouse. Diabetes 32:1152–1161
32. Spritz N, Singh H, Mariman B (1975) Decrease in myelin con-

tent of rabbit nerve with aging and diabetes. Diabetes 24:680–683
33. Stewart MA, Sherman WR, Anthony S (1966) Free sugars in alloxan diabetic nerve. Biochem Biophys Res Commun 22:488–491
34. Sugimura K, Dyck PJ (1980) Multifiber fiber loss in proximal sciatic nerve in symmetric distal diabetic neuropathy. J Neurol Sci 53:501–509
35. Thomas PK, Lascelles RG (1966) The pathology of diabetic neuropathy. Q J Med 35:489–509
36. Thomas PK, Elliason S (1984) Diabetic neuropathy. In: Dyck PJ, Thomas PK, Lambert EH (eds) Peripheral neuropathy, chap 76. Saunders, Philadelphia, PA, pp 1776–1810
37. Vital C, Brechenmacher C, Servise JM, Bellance R, Vital A, Dartigues JF, Boissieras P (1983) Ultrastructural study of peripheral nerve in arteritic diabetic patents. Acta Neuropathol (Berl) 61:225–231
38. Vracko R (1982) A comparison of the microvascular lesions in diabetes mellitus with those of normal aging. J Am Geriatr Soc 30:201–205
39. Yagihashi S, Matsunaga M (1979) Ultrastructural pathology of peripheral nerves in patients with diabetic neuropathy. Tohoku J Exp Med 129:357–366

Received May 4, 1984 / Accepted July 20, 1984